Supplemental Information

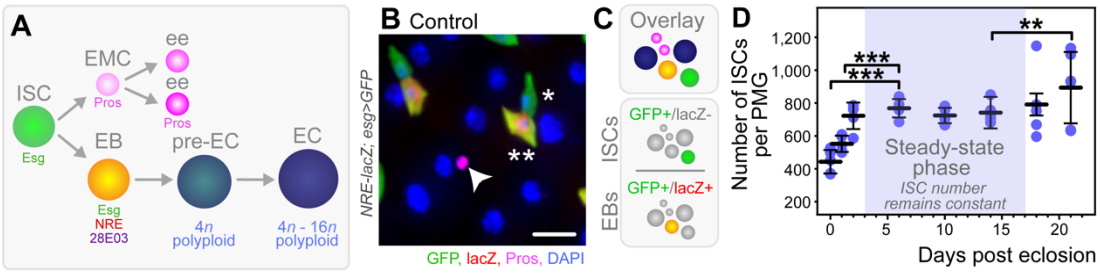

Figure S1. The Number of ISCs Remains at a Steady-State in Young Flies, Related to Figure 1

(A) Schematic representation of the lineage and cell-specific markers of each cell type within the *Drosophila* posterior midgut (PMG).

(B) Image illustrating all cell types in the PMG of flies at 7 days post eclosion (PE) with cell-specific markers outlined in (A) (ISC, asterisk; EB, double asterisks; ee, arrow head; ECs, polyploid). Scale bar = 20 μm.

(C) Protocol used to quantify the number of ISCs per PMG. Using flies of the genotype *NRE-lacZ; esg>GFP;,* ISC number was determined by subtracting the number of diploid EBs (lacZ+ cells) from the number of diploid ISCs and EBs (GFP+ cells).

(D) Quantification of the number of ISCs per PMG over time. The total number of ISCs per PMG increased in the first three days PE, remained at a steady state average of 745 ± 56 from 3 to 17 days PE, and subsequently increased in aging flies. $n = 5$. (***) denotes $p < 0.001$.

(B-D) *NRE-lacZ; esg>GFP;*

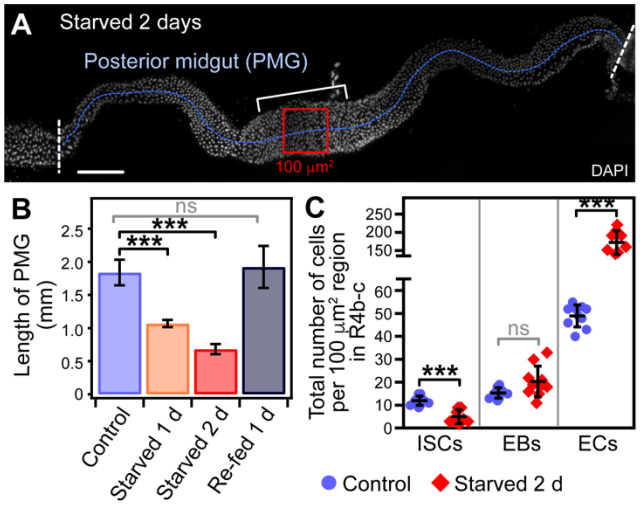

Figure S2. The Posterior Midgut Shortens upon Starvation, Inducing Severe Cellular Over-crowding and Loss of ISCs, Related to Figure 1

(A) Representation of methods used to quantify the length of the PMG (blue dashed line) and to quantify the total number of cells per 100 μm x 100 μm region in the center of R4b-c (red box) (bracket denotes area of muscle contraction). Scale bar = 100 μm.

(B) Quantification of the length of the PMG from sibling control, starved, and starved and re-fed flies. The PMG rapidly shortened in starved flies to approximately one-half the length of controls. Upon re-feeding, the length of the PMG recovered to that of controls. n = 10. (***) denotes $p <$ 0.001.

(C) Quantification of the total number of each cell type per 100 μm x 100 μm region in the center of R4b-c, the area of severe cellular over-crowding, of starved flies. The number of ISCs significantly decreased per region, while the number of ECs significantly increased per region. n = 10. (***) denotes $p < 0.001$.

(A-C) *NRE-lacZ; esg>GFP;*

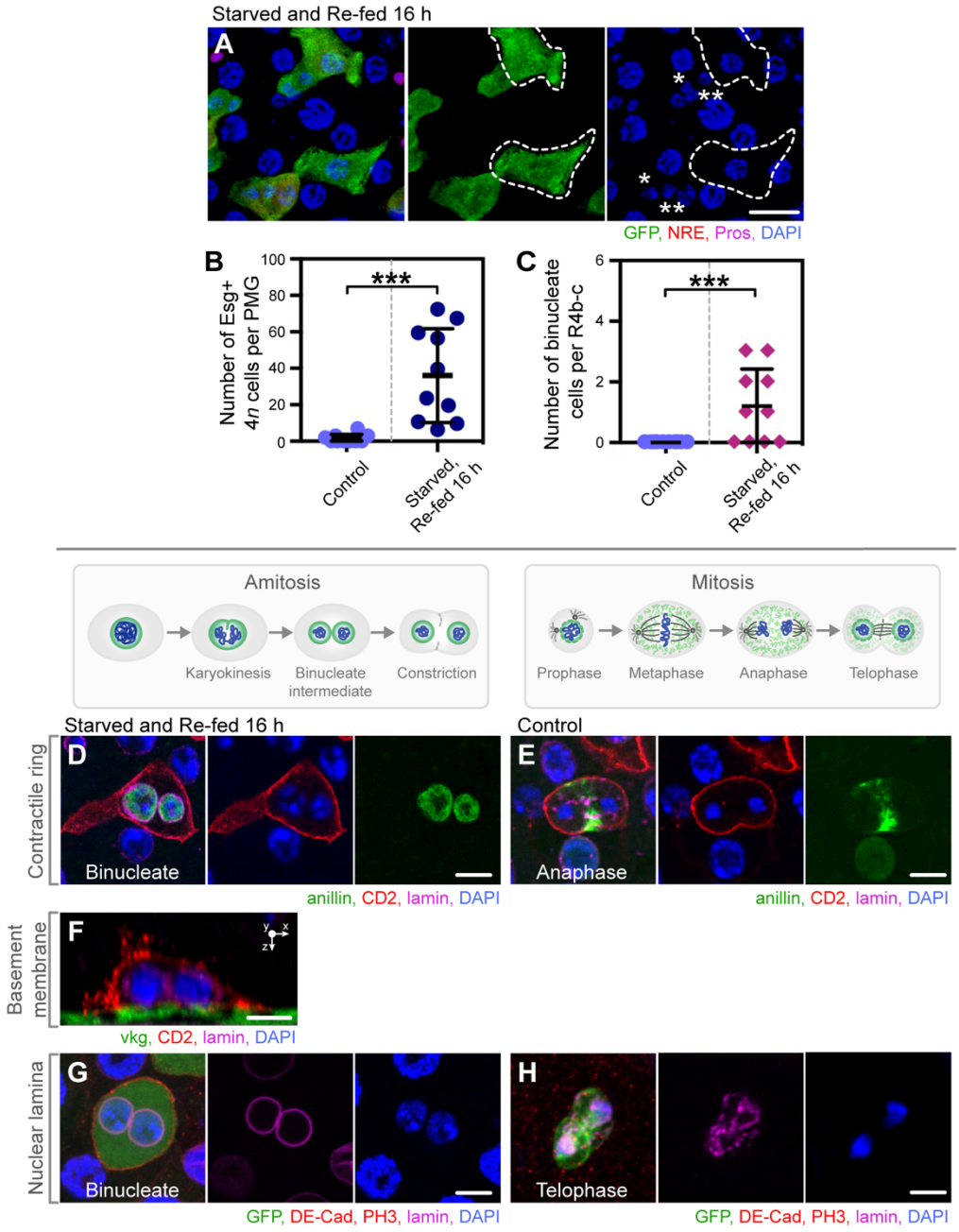

Figure S3. Polyploid Cells Undergoing Amitosis are Observed in Animals that were Starved and Re-fed for 8-16 hours, Related to Figure 3

(A) Image of a representative region in R4b-c of a fly that was starved and re-fed for 16 hours. *esg-GAL4*-driven GFP expression is observed in a subset of polyploid cells (white dashed outline) in addition to ISCs (asterisk) and EBs (double asterisk). Scale bar = 20 μm.

(B) Quantification of the number of Esg+ 4*n* cells per PMG. $n = 10$. (***) denotes $p < 0.001$.

(C) Quantification of the number of binucleate amitotic cells per PMG. $n = 10$. (***) denotes $p < 0.001$.

(D-E) Images of anillin localization in a representative binucleate polyploid cell undergoing amitosis in R4b-c of a fly that was starved and re-fed for 16 hours (D), in contrast to a mitotic cell in anaphase (E). Anillin was restricted to the nucleus of amitotic cells, as opposed to localization to the contractile ring of mitotic cells in late anaphase. Scale bar = 10 μm.

(F) Image of a representative binucleate polyploid cell undergoing amitotis in R4b-c of a fly that was starved and re-fed for 16 hours. Amitotic cells are laminated to the basement membrane, represented by *viking (vkg)-GFP*. Scale bar = 10 μm.

(G-H) Images of a representative binucleate polyploid cell undergoing amitosis in R4b-c of a fly that was starved and re-fed for 16 hours (G), in contrast to a mitotic cell in telophase (H). Scale bar = 10 μm.

(A, G-H) *NRE-lacZ; esg>GFP;*

(B-C) *NRE-lacZ; esg>CD2;*

(D-E) *UAS-anillin-GFP; esg>CD2;*

(F) *NRE-lacZ; esg>CD2, vkg-GFP;*

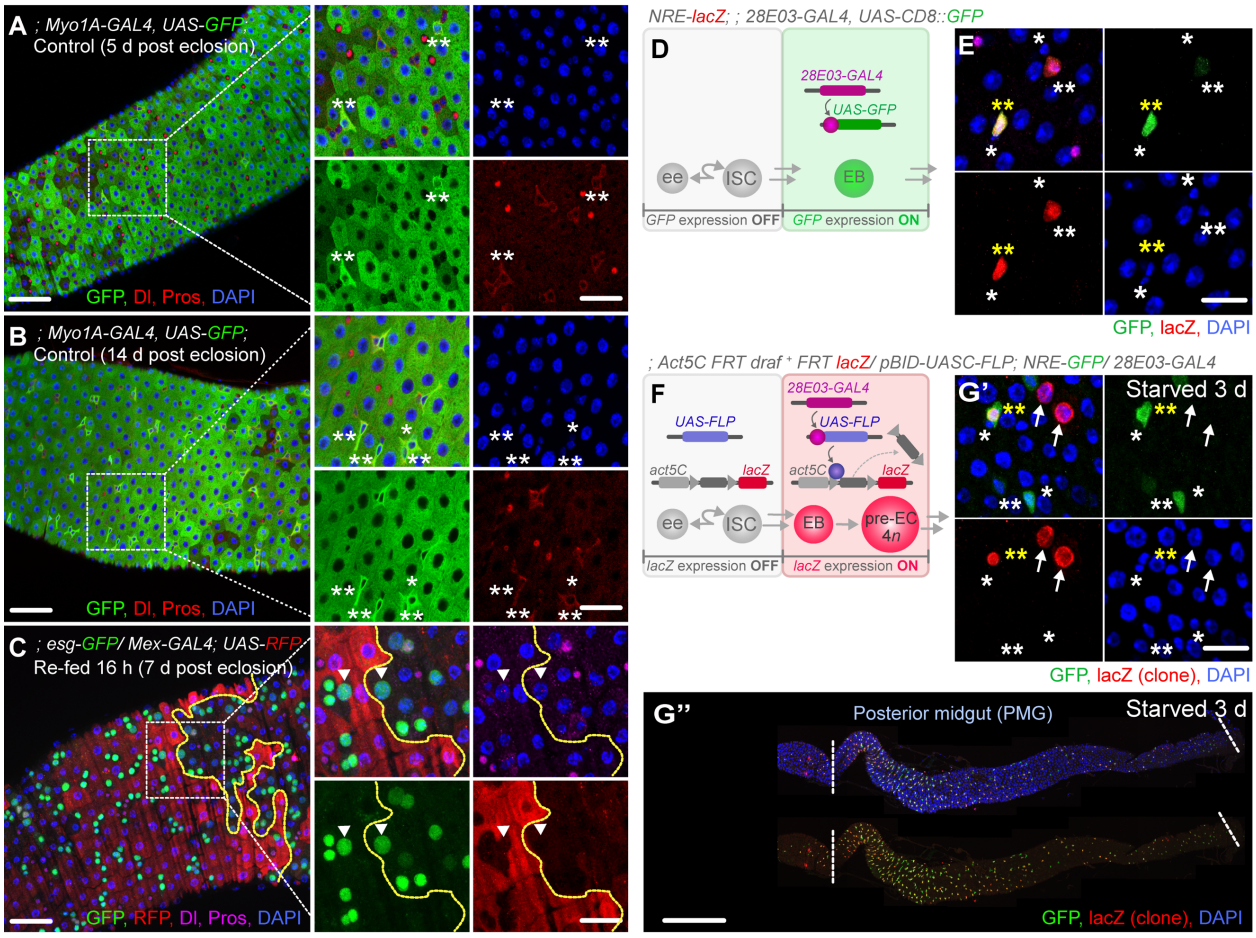

Figure S4. The EC-lineage Specific Driver *28E03-GAL4* is Used to Determine the Contribution of cells in the EC-lineage to ISC Replacement, Related to Figure 4

(A-B) Images of *Myo1A-GAL4*-driven reporter expression in control flies. *Myo1A-GAL4* becomes non-EC specific with age, with marked progenitor cells observed as early as 5 d PE (A, double asterisk) and pairs of ISCs and EBs observed at 14 d PE (B, asterisk and double asterisk). The non-specificity of *Myo1A-GAL4* deems this driver inappropriate for stringent lineage analysis. Scale bar = 50 μm (left panels), 20 μm (right panels).

(C) Images of *Mex-GAL4*-driven reporter expression in flies that were starved and re-fed for 16 hours. *Mex-GAL4* is specifically expressed in ECs. However, it is largely absent from ECs in R4b-c of the posterior midgut (right of dotted yellow line), where the majority of ISCs are lost with starvation. In addition, *Mex-GAL4*-driven reporter expression does not overlap with Esg+ polyploid cells (arrow head, right panels). Therefore, this driver is not appropriate for use in our lineage analysis. Scale bar = 50 μm (left panels), 20 μm (right panels).

(D) Schematic representation of *28E03-GAL4*-driven reporter expression.

(E) Images of *28E03-GAL4* reporter expression in control flies. *28E03-GAL4* drives reporter expression in a subset of EBs marked with *NRE-lacZ* (yellow double asterisk denotes co-expression with *NRE-lacZ*). *28E03-GAL4*-driven reporter expression is absent in all ISCs (white asterisks) of the PMG. Scale bar = 20 μm.

(F) Schematic representation of the flipout system used to determine the contribution of cells in the EC-lineage to ISC replacement. A stop cassette flanked by *FRT* sites is excised upon expression of *flippase* (*FLP*) using the GAL4/UAS system and the EC-lineage-specific driver, *28E03-GAL4*.

(G) Images of *28E03-GAL4*-driven flipout clones marking the EC-lineage in starved flies, as observed by Act5C-lacZ positive EBs (G', yellow double asterisks) and polyploid ECs (G', arrows). No ISCs (G', white asterisks) were lineage-labeled in starved flies, confirming that starvation does not induce *28E03-GAL4* expression in ISCs. As the efficiency of flipout was low, only a subset of cells in the EC-lineage were labeled. Scale bar = 20 μm (G'), 100 μm (G'').

(A-B) *; Myo1A>GFP;*

(C) *; esg-GFP/MexGAL4; +/UAS-RFP*

(D-E) *NRE-lacZ; ; 28E03>CD8::GFP*

(F-G") *w ; Act5C FRT draf+ FRT lacZ/ pBID-UASC-FLP; NRE-GFP/28E03-GAL4*

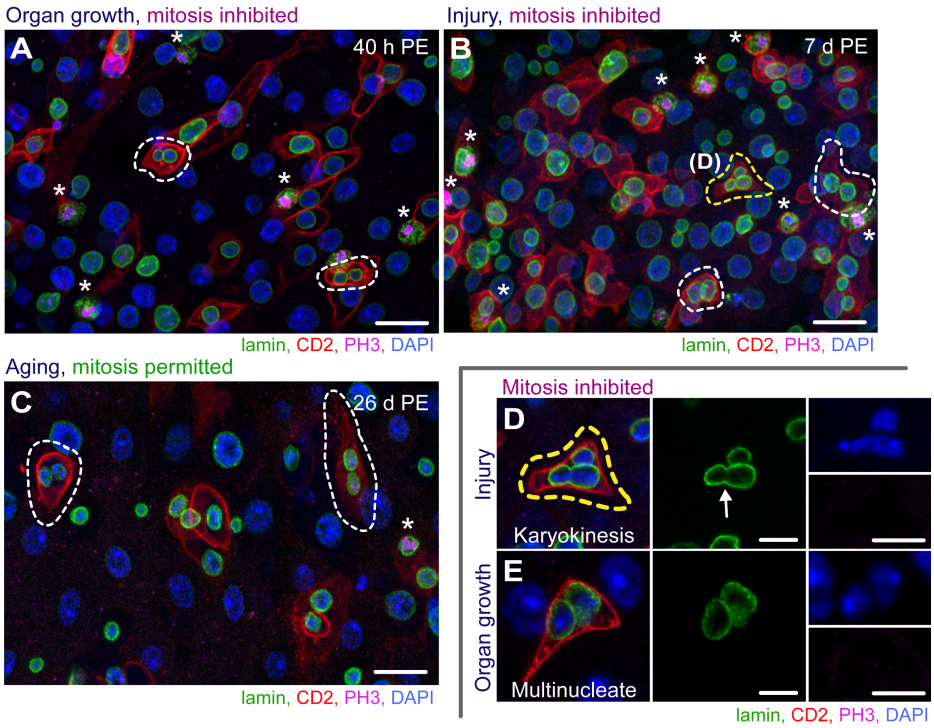

Figure S5. Amitosis Occurs in Regions Where Nearly all ISCs are Stalled in Mitosis, Related to Figure 6

(A-B) Images of representative regions within the PMG of newly eclosed (A) or injured (B) flies treated with demecolcine. Amitosis occurred only in regions in which the majority of ISCs were stalled in mitosis as a consequence of demecolcine treatment. Scale bar = 20 μm.

(C) Image of a representative region within the PMG of an aging fly (26 d PE). Amitosis was observed even in the absence of demecolcine treatment, suggesting that ISCs become dysfunctional with age or that amitosis is occurring in response to potential ISC loss at this age. Scale bar = 20 μm.

(D-E) Images of representative amitotic cells in injured adult flies (D) and newly eclosed flies (E) in which mitosis was inhibited. Amitotic figures that appeared to be undergoing a second karyokinesis event (D) and that were trinucleate (E) were observed, suggesting that the process of amitosis can be error-prone in this tissue. Scale bar = 10 μm.

(A-D) ISCs stalled in mitosis, asterisks; binucleate cell, white dotted outline; trinucleate cell, yellow dotted outline.

(A-E) *NRE-lacZ; esg>CD2;*